Interaction and Multiscale Mechanics, Vol. 1, No. 3 (2008) 357-368 357
DOI: http://dx.doi.org/10.12989/imm.2008.1.3.357

Multi-type sensor placement design for damage detection

Y. Q. Li

Department of Engineering Mechanics, Tsinghua University, Beijing, 100084, China

M. S. Zhou

CCCC Highway and Bridge Consultants Co., Ltd, China

Z. H. Xiang* and Z. Z. Cen

Department of Engineering Mechanics, Tsinghua University, Beijing, 100084, China

(Received January 30, 2008, Accepted July 8, 2008)

Abstract. The result of damage detection from on-site measurements is commonly polluted by unavoidable measurement noises. It is widely recognized that this side influence could be reduced to some extent if the sensor placement was properly designed. Although many methods have been proposed to find the optimal number and location of mono-type sensors, the optimal layout of multi-type sensors need further investigation, because a network of heterogeneous sensors is commonly used in engineering. In this paper, a new criterion of the optimal placement for different types of sensors is proposed. A corresponding heuristic is developed to search for good results. In addition, Monte Carlo simulation is suggested to design a robust damage detection system which contains certain redundancies. The validity of these methods is illustrated by two bridge examples.

Keywords: damage detection; sensor placement; bridge.

1. Introduction

During the past years, much attention has been drawn on damage detection techniques which play an important role in Structural Health Monitoring Systems (Sohn *et al*. 2003). Because damage detection is a kind of inverse problem, it is usually ill-posed. That means small measurement noises could lead to severe detection errors if the measuring system and damage detection algorithms were not properly designed. To improve the well-posedness of damage detection procedure, at least two approaches have been tried: one is using *a priori* information to regularize the procedure (Yusuke *et al*. 1994, Zhou *et al*. 2007); another is carefully designing the layout of sensors (Kammer 1991, Heo *et al*. 1997, Haftka and Scott 1998, Padula and Kincaid 1999, Li *et al*. 2000, Worden and Burrows 2001, Xiang *et al*. 2003). This paper discusses the second approach.

* Corresponding Author, Email: xiangzhihai@tsinghua.edu.cn

So far, many methods have been proposed to find the optimal sensor placement (Kammer 1991, Heo *et al*. 1997, Haftka and Scott 1998, Padula and Kincaid 1999, Li *et al*. 2000, Worden and Burrows 2001, Xiang *et al*. 2003). These methods usually consist of a criterion of the optimality and a combinatorial optimization algorithm. Most popular criteria are more or less related with certain properties of Fisher Information Matrix (FIM) $\boldsymbol{J}^T\boldsymbol{J}$, where $\boldsymbol{J}$, called Jacobian matrix, is the derivation of measurements over damage parameters. Based on these criteria, simple heuristics (Kammer 1991, Heo *et al*. 1997, Xiang *et al*. 2003) as well as modern meta-heuristics, e.g., Genetic Algorithm (GA), Simulated Annealing (SA) and Tabu Search (TS) (Li *et al*. 2000, Worden and Burrows 2001) etc., have been adopted to find the 'optimal' sensor placement.

Although many researches have been conducted in this field, most of them discuss only the optimal number and location of mono-type sensors. But in engineering, a network of heterogeneous sensors is commonly used to measure different kinds of variables. For example, displacements and strains can be easily measured, and consequently, it is natural to conduct damage detection based on these two kinds of measurements (Sanayei and Onipede 1991, Banan and Hjelmstad 1994, Banan and Hjelmstad 1994, Liu and Chian 1997, Cui *et al*. 2000). Therefore, it is important to study the optimal sensor placement under this circumstance.

By tracing the propagation of measurement errors, this paper proposes a new criterion of the optimal placement for different types of sensors. A new heuristic incorporated in Monte Carlo simulation is also developed to design a robust damage detection system which contains certain redundancies. The validity of these methods is illustrated by two bridge examples.

2. The damage detection method

Since damage can be regarded as the reduction of structural stiffness, the damage detection is actually a kind of stiffness parameter identification problem based on measured structural responses. It can conventionally take the Young's modulus as the stiffness parameter, which can be identified by measured displacements and strains through the following nonlinear optimization formulation with least-squares objective:

$$\begin{aligned} &\text{Minmize:} \quad f(\boldsymbol{p}) = \boldsymbol{R}^T\boldsymbol{R} \\ &\text{Subjected to: } \boldsymbol{K}(\boldsymbol{p})\boldsymbol{u} = \boldsymbol{F} \\ &\boldsymbol{p} \in \boldsymbol{D}_p \end{aligned} \tag{1}$$

where $\boldsymbol{K}$ is the stiffness matrix, which can be easily formulated in the Finite Element (FE) method; $\boldsymbol{u}$ is the vector of general displacements and strains; $\boldsymbol{F}$ is the load vector; $\boldsymbol{p}$ is the parameter vector of Young's modulus to be identified; $\boldsymbol{D}_p$ is the admissible set of $\boldsymbol{p}$; and $\boldsymbol{R}$ is the residual vector, which is defined as:

$$\boldsymbol{R}(\boldsymbol{p}) = \boldsymbol{u}_s^* - \boldsymbol{S}\boldsymbol{u} \tag{2}$$

where $\boldsymbol{u}_s^*$ are measured displacements and strains; $\boldsymbol{S}$ is a Boolean matrix which specifies the number and location of measurements.

Eq. (1) can be efficiently solved by using Gauss-Newton iteration method. According to Xiang *et al*. (2003), the iteration procedure is:

$$\boldsymbol{p}^{n+1} = \boldsymbol{G}(\boldsymbol{p}^n) \equiv \boldsymbol{p}^n - [(\boldsymbol{J}^n)^{\mathrm{T}}\boldsymbol{J}^n]^{-1}(\boldsymbol{J}^n)^{\mathrm{T}}\boldsymbol{R}^n \qquad n = 0, 1, 2, \ldots \tag{3}$$

where n is the iteration step; $\boldsymbol{G}$ is the mapping function; $\boldsymbol{J}$ is the Jacobian matrix; and $\boldsymbol{J}^{\mathrm{T}}\boldsymbol{J}$ is the FIM.

It is noticed that above formulations are the same as those of parameter identification with mono-type sensors (Xiang *et al*. 2003).

3. The optimal placement of multi-type sensors

The design of optimal sensor placement is a combinatorial optimization problem, where the criterion of optimality and the corresponding optimization algorithm are two critical factors.

3.1 The criterion of optimality

The criterion of optimality can be deduced by tracing the propagation of measurement errors during the parameter identification procedure. It is supposed that the initial parameter $\boldsymbol{p}^0$ contains a bias $\delta\boldsymbol{p}$ with respect to the true parameter $\boldsymbol{p}^*$:

$$\boldsymbol{p}^0 = \boldsymbol{p}^* + \delta\boldsymbol{p} \tag{4}$$

It is also supposed that the measurements contain absolute errors ε:

$$\boldsymbol{u}_s^* = \boldsymbol{S}(\boldsymbol{u}^* + \varepsilon) \tag{5}$$

The difference of $\boldsymbol{p}^n$ to $\boldsymbol{p}^*$ at iteration step n can be evaluated as:

$$\boldsymbol{h}^n = \boldsymbol{p}^n - \boldsymbol{p}^* \qquad n = 0, 1, 2, \ldots \tag{6}$$

From Eqs. (2) through (6), it reads:

$$\boldsymbol{h}^n - \boldsymbol{h}^{n-1} = \boldsymbol{p}^n - \boldsymbol{p}^{n-1} = \boldsymbol{G}(\boldsymbol{p}^{n-1}) - \boldsymbol{p}^{n-1} = [\boldsymbol{\Omega}(\boldsymbol{p}^{\zeta_{n-1}}, \boldsymbol{\varepsilon}^{\zeta_{n-1}}) - \boldsymbol{I}]\boldsymbol{h}^{n-1} - [(\boldsymbol{J}^{\mathrm{T}}\boldsymbol{J})^{-1}\boldsymbol{J}^{\mathrm{T}}\boldsymbol{S}]_{\boldsymbol{p} = \boldsymbol{p}^{\xi_{n-1}}}\boldsymbol{\varepsilon}$$

$$\boldsymbol{h}^n = \boldsymbol{\Omega}(\boldsymbol{p}^{\zeta_{n-1}}, \boldsymbol{\varepsilon}^{\zeta_{n-1}})\boldsymbol{h}^{n-1} + \boldsymbol{A}(\boldsymbol{p}^{\zeta_{n-1}})\boldsymbol{\varepsilon} \tag{7}$$

where $\boldsymbol{p}^{\zeta_{n-1}} = \boldsymbol{p}^* + \beta(\boldsymbol{p}^{n-1} - \boldsymbol{p}^*), 0 < \beta < 1, \boldsymbol{\varepsilon}^{\zeta_{n-1}} \in (0, \boldsymbol{\varepsilon})$, and

$$\boldsymbol{\Omega}(\boldsymbol{p}, \boldsymbol{\varepsilon}) \equiv \frac{\partial \boldsymbol{G}(\boldsymbol{p}, \boldsymbol{\varepsilon})}{\partial \boldsymbol{p}} = (\boldsymbol{J}^{\mathrm{T}}\boldsymbol{J})^{-1}\frac{\partial(\boldsymbol{J}^{\mathrm{T}}\boldsymbol{J})}{\partial \boldsymbol{p}}(\boldsymbol{J}^{\mathrm{T}}\boldsymbol{J})^{-1}\boldsymbol{J}^{\mathrm{T}}\boldsymbol{R} - (\boldsymbol{J}^{\mathrm{T}}\boldsymbol{J})^{-1}\frac{\partial \boldsymbol{J}^{\mathrm{T}}}{\partial \boldsymbol{p}}\boldsymbol{R} \tag{8}$$

$$\boldsymbol{A}(\boldsymbol{p}) \equiv (\boldsymbol{J}^{\mathrm{T}}\boldsymbol{J})^{-1}\boldsymbol{J}^{\mathrm{T}}\boldsymbol{S} \tag{9}$$

Define:

$$L_{\Omega} \equiv \mathrm{Max}\|\boldsymbol{\Omega}(\boldsymbol{p}, \boldsymbol{\varepsilon})\|_{\infty} \tag{10}$$

$$L_A \equiv \|\boldsymbol{A}(\boldsymbol{p})\boldsymbol{\varepsilon}\|_{\infty} \tag{11}$$

From Eqs. (7), (10) and (11), the following relation is valid:

$$\|\boldsymbol{h}^n\|_\infty \le L_\Omega \|\boldsymbol{h}^{n-1}\|_\infty + L_A \le L_\Omega^2 \|\boldsymbol{h}^{n-2}\|_\infty + (1+L_\Omega)L_A \cdots \le L_\Omega^n \|\delta \boldsymbol{p}\|_\infty + (1 + L_\Omega + \cdots L_\Omega^{n-1})L_A \quad (12)$$

If $L_\Omega < 1$, then

$$\lim_{n\to\infty}\|\boldsymbol{h}^n\|_\infty \le \frac{1}{1-L_\Omega}L_A \approx L_A(1+L_\Omega) \quad (13)$$

The iteration procedure converges to a solution with bias:

$$B \equiv L_A(1+L_\Omega) \quad (14)$$

This is coincident with the requirement of well-posedness presented in Xiang *et al*. (2003).

The above analysis reveals that if $L_\Omega < 1$, the parameter identification procedure will converge to a unique solution with bias B. Since L_Ω and L_A contain $\boldsymbol{S}$, the sensor placement should be optimized so that $L_\Omega < 1$ and B reaches a minimum value. This criterion of optimal sensor placement is similar to the one proposed in Xiang *et al*. (2003), however, multi-type sensors are involved here and absolute measurement errors are considered instead of relative measurement errors.

In Eq. (8), $\boldsymbol{\Omega}$ can be evaluated by applying the Taylor expansion with respect to $\boldsymbol{p}^*$ and $\boldsymbol{\varepsilon}$:

$$\boldsymbol{\Omega}(\boldsymbol{p}, \boldsymbol{\varepsilon}) \approx \boldsymbol{\Omega}(\boldsymbol{p}^*, \boldsymbol{0}) + \frac{\partial \boldsymbol{\Omega}(\boldsymbol{p}^*, \boldsymbol{0})}{\partial \boldsymbol{p}}(\boldsymbol{p}-\boldsymbol{p}^*) + \frac{\partial \boldsymbol{\Omega}(\boldsymbol{p}^*, \boldsymbol{0})}{\partial \boldsymbol{\varepsilon}}\boldsymbol{\varepsilon} \quad (15)$$

Denoting

$$\boldsymbol{C}(\boldsymbol{p}^*) \equiv \frac{\partial \boldsymbol{\Omega}(\boldsymbol{p}^*, \boldsymbol{0})}{\partial \boldsymbol{p}} = [(\boldsymbol{J}^*)^{\mathrm{T}}\boldsymbol{J}^*]^{-1}(\boldsymbol{J}^*)^{\mathrm{T}}\frac{\partial \boldsymbol{J}^*}{\partial \boldsymbol{p}} \quad (16)$$

$$\boldsymbol{D}(\boldsymbol{p}^*) \equiv \frac{\partial \boldsymbol{\Omega}(\boldsymbol{p}^*, \boldsymbol{0})}{\partial \boldsymbol{\varepsilon}} = -[(\boldsymbol{J}^*)^{\mathrm{T}}\boldsymbol{J}^*]^{-1}\left\{\frac{\partial (\boldsymbol{J}^*)^{\mathrm{T}}}{\partial \boldsymbol{p}} - \frac{\partial[(\boldsymbol{J}^*)^{\mathrm{T}}\boldsymbol{J}^*]}{\partial \boldsymbol{p}}[(\boldsymbol{J}^*)^{\mathrm{T}}\boldsymbol{J}^*]^{-1}(\boldsymbol{J}^*)^{\mathrm{T}}\right\}\boldsymbol{S} \quad (17)$$

and observing

$$\boldsymbol{\Omega}(\boldsymbol{p}^*, \boldsymbol{0}) = \boldsymbol{0} \quad (18)$$

it obtains:

$$\|\boldsymbol{\Omega}(\boldsymbol{p}, \boldsymbol{\varepsilon})\|_\infty \le \|\boldsymbol{C}(\boldsymbol{p}^*)\|_\infty \|\boldsymbol{p}-\boldsymbol{p}^*\|_\infty + \|\boldsymbol{D}(\boldsymbol{p}^*)\boldsymbol{\varepsilon}\|_\infty \quad (19)$$

Therefore,

$$L_\Omega \approx \|\boldsymbol{C}(\boldsymbol{p}^*)\|_\infty \|\delta \boldsymbol{p}\|_\infty + \|\boldsymbol{D}(\boldsymbol{p}^*)\boldsymbol{\varepsilon}\|_\infty \quad (20)$$

Similarly,

$$\boldsymbol{A}(\boldsymbol{p}) \approx \boldsymbol{A}(\boldsymbol{p}^*) + \frac{\partial \boldsymbol{A}(\boldsymbol{p}^*)}{\partial \boldsymbol{p}}(\boldsymbol{p}-\boldsymbol{p}^*) = \boldsymbol{A}(\boldsymbol{p}^*) + \boldsymbol{D}(\boldsymbol{p}^*)(\boldsymbol{p}-\boldsymbol{p}^*) \quad (21)$$

$$\|\boldsymbol{A}(\boldsymbol{p})\|_\infty \le \|\boldsymbol{A}(\boldsymbol{p}^*)\|_\infty + \|\boldsymbol{D}(\boldsymbol{p}^*)\|_\infty \|\boldsymbol{p}-\boldsymbol{p}^*\|_\infty \le \|\boldsymbol{A}(\boldsymbol{p}^*)\|_\infty \|\boldsymbol{D}(\boldsymbol{p}^*)\|_\infty \|\delta \boldsymbol{p}\|_\infty \quad (22)$$

$$L_A \approx \|\boldsymbol{A}(\boldsymbol{p})\|_\infty + \|\boldsymbol{D}(\boldsymbol{p}^*)\|_\infty \|\delta \boldsymbol{p}\|_\infty \quad (23)$$

3.2 The optimization algorithm

The design of optimal sensor placement is a combinatorial optimization problem, which is very time consuming if the number of variables is large. Therefore, certain heuristics are commonly used to get near optimal solutions for practical problems. The heuristics could be very simple, such as the Effective Independence Method (EIM) proposed by Kammer (1991), but the result is not so satisfactory. Better results could be obtained if meta-heuristics are adopted, such as the GA, SA and TS (Worden and Burrows 2001). However, there are some empirical parameters need to be tuned in meta-heuristics, which are usually case sensitive. Another shortcoming of meta-heuristics is the lack of stopping criterion, therefore, the number of iterations is also empirically specified.

In this paper, a new heuristic is proposed by adding more local searches in the EIM to get better results while keeping the efficiency of the algorithm. This heuristic contains a hierarchy of local searches organized as follows:

(1) Put all candidate measurements into set $\boldsymbol{S}_1$. Calculate the corresponding bias $B(\boldsymbol{S}_1)$ and L_Ω. If $L_\Omega < 1$, keep $\boldsymbol{S}_1$ as the best measurement set $\boldsymbol{S}$;

(2) Try to remove one measurement from $\boldsymbol{S}_1$. If $B(\boldsymbol{S}_1)$ is reduced, put this measurement into set $\boldsymbol{S}_2$. This process continues until every measurement in $\boldsymbol{S}_1$ has been tested. Update the best measurement set $\boldsymbol{S}$, if the L_Ω of $\boldsymbol{S}_1$ is less than one and $B(\boldsymbol{S}_1)$ is the minimum;

(3) Try to remove consecutive two measurements from $\boldsymbol{S}_1$. If $B(\boldsymbol{S}_1)$ is reduced, put these two measurements into set $\boldsymbol{S}_2$. This process continues until every consecutive two measurements in $\boldsymbol{S}_1$ have been tested. Update the best measurement set $\boldsymbol{S}$, if the L_Ω of $\boldsymbol{S}_1$ is less than one and $B(\boldsymbol{S}_1)$ is the minimum;

(4) Exchange each pair of measurements between $\boldsymbol{S}_1$ and $\boldsymbol{S}_2$. Update the best measurement set $\boldsymbol{S}$, if the L_Ω of $\boldsymbol{S}_1$ is less than one and $B(\boldsymbol{S}_1)$ is the minimum. If the best measurement set $\boldsymbol{S}$ has been successfully updated once, go to step (2), otherwise stop the heuristic.

From the above heuristic, the number and location of each type of sensor can be automatically determined. However, it is very difficult to estimate the bias $\boldsymbol{\delta p}$ in Eq. (4), because $\boldsymbol{p}^*$ is unknown in the design phase. Therefore, Monte Carlo simulation is adopted to obtain the candidate good measurements. For each sample of simulation, let $\boldsymbol{\delta p} = \boldsymbol{0}$, and $\boldsymbol{p}^0$ (assumed as $\boldsymbol{p}^*$) is randomly generated following the Gauss distribution. The $\boldsymbol{\varepsilon}$ takes the tolerance of the sensors with randomly assigned sign. The final sensor placement is the union of the subset of resulted $\boldsymbol{S}$ of each sample from the above heuristic. This subset contains the measurements whose Occurrence Probability (OP) over all samples exceeds a specified value. In this way, a reasonable sensor placement can be constructed and the redundancy is also naturally considered.

The sensor placement obtained through the above algorithm is a super set of $\boldsymbol{S}$ over all samples. There is no quarantine that it is the best placement for the true problem. However, what can be ensured is that the best placement is a subset of this super set if the OP is relatively low and the heuristic can find the optimal result. Therefore, during the damage detection procedure the best sensor placement should be re-optimized from this super set according to an initial parameter $\boldsymbol{p}^0$, using the same heuristic. To remove the side effect of empirically specifying $\boldsymbol{p}^0$, an algorithm similar to what suggested in Ref. (Li *et al.* (DOI: 10.1002/cnm.1052)) is proposed here. In this algorithm, the sensor placement design and the parameter identification are alternatively conducted as follows:

(a) Empirically specify $\boldsymbol{p}^0$. Set $n = 1$ and $\boldsymbol{S}^{n-1}$ as an empty set;

(b) Based on $\boldsymbol{p}^{n-1}$, use the heuristic to find a good sensor placement $\boldsymbol{S}^n$;

(c) If $\boldsymbol{S}^n = \boldsymbol{S}^{n-1}$, stop. Otherwise, go to next step;

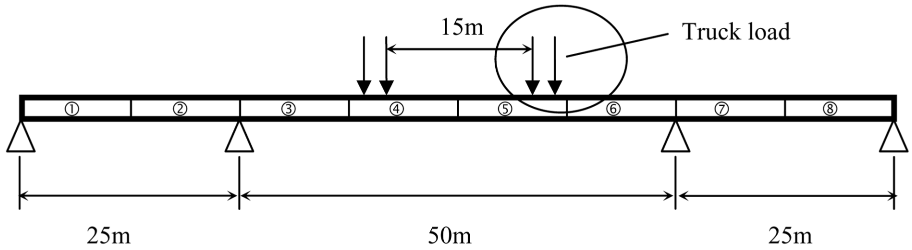

Fig. 1 A three-span continuous beam bridge

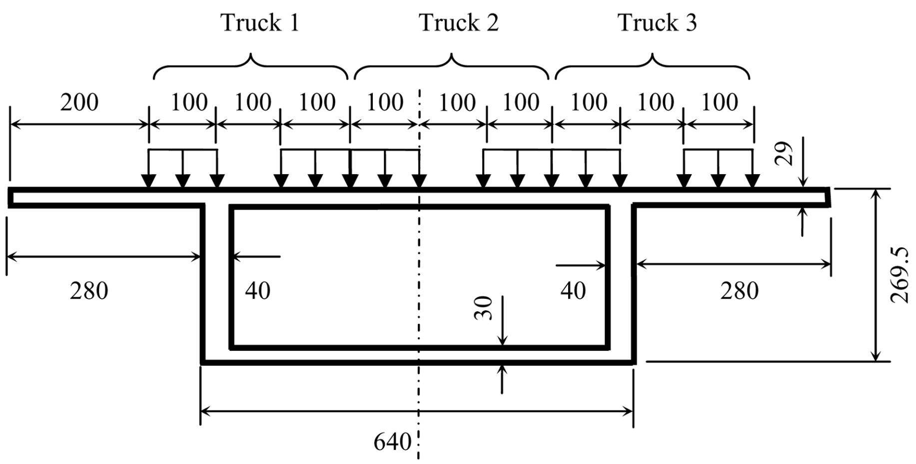

Fig. 2 The cross-section of the box beam and the distribution of truck load (unit is in cm)

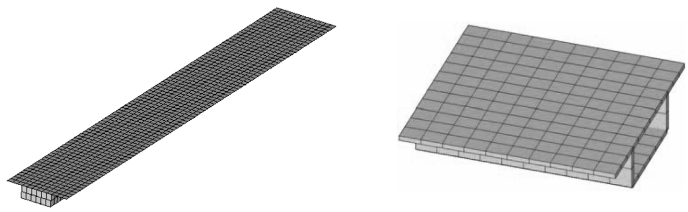

Fig. 3 The FE model

(d) Based on $\boldsymbol{S}^n$, identify the parameter $\boldsymbol{p}^n$;

(e) Set $n = n + 1$, go to (b).

In this way, the sensor placement is dynamically updated.

4. Examples

As Fig. 1 shows, the model of a three-span continuous beam bridge is taken as an example to illustrate the validity of the algorithms proposed in this paper. Because it is a box beam (see Fig. 2), four-node shell FE is used to model this structure (see Fig. 3).

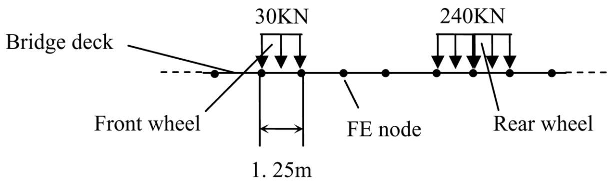

Fig. 4 The detail of truck load in Fig. 1

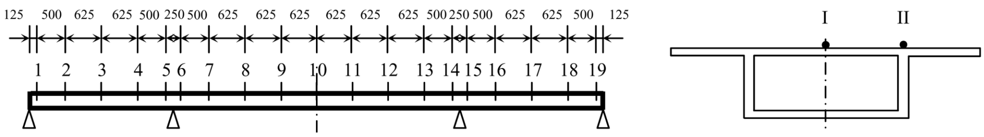

Fig. 5 The candidate displacement measurements (unit in cm)

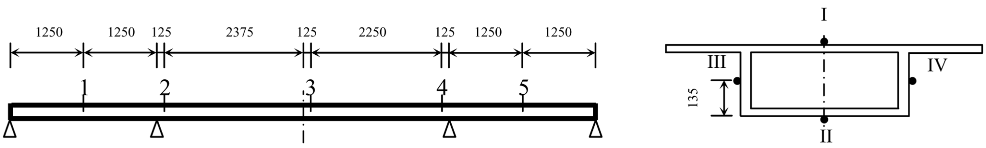

Fig. 6 The candidate strain measurements (unit in cm)

A simulated truck loading is applied to calculate displacements and strains, which are taken as 'measurements'. As Figs. 1 and 4 show, two rows of truck loads are applied symmetrically about the center line of middle span. Each row has three truck loads aligned unsymmetrically along the width of the bridge deck (see Fig. 2). As Fig. 4 illustrates, the weight of each front wheel is 30 KN, and the weight of each rear wheel set is 240KN. These loads are averaged over the element they occupy, i.e., effective pressures are applied on the bridge deck.

As Fig. 5 shows, there are 38 deflections taken as candidate displacement 'measurements'. These 'measurements' are distributed on 19 cross-sections and each section has two 'measurements'. Fig. 6 depicts the distribution of strain 'measurements'. It assumed that strain gauges are installed on five cross-sections, each cross-section measures four strains in the length direction of the bridge.

It is assumed that only the Young's modulus is reduced in the damaged state, while the geometry keeps unchanged. Therefore, Young's moduli of eight segments (see Fig. 1) are identified as the damage parameters. In following examples, suppose the Young's modulus of all sections is 35GPa in the intact state.

4.1 The benefit from using displacements together with strains

In this example, the true values of Young's modulus are used to design the sensor placement. The true displacements and strains of the intact state are taken from FE results, from which two sets of 'measurements' are generated according to sensor tolerances: 0.01 mm for displacements and 1 μ for strains. In Set 1, all measurements are polluted with positive noises and in Set 2, only the signs of noises are randomly determined. For each measurement set, three cases are tested: only pure displacements are considered in Case 1; only pure strains are considered in Case 2; and both displacements and strains are considered in Case 3.

Table 1 Optimal sensor placement of three cases

Measurement		Set 1			Set 2		
		Case 1	Case 2	Case 3	Case 1	Case 2	Case 3
Displacement	I	5, 7, 9, 11, 13, 15	/	5, 7, 9, 11, 13, 15	3, 4, 9, 10, 12, 15, 16	/	3, 4, 6, 8, 9, 10, 12, 15, 16
	II	3, 9, 11, 17	/	3, 9, 11, 17	3, 4, 5, 6, 8, 10, 11, 17, 18	/	3, 4, 6, 10, 11, 17, 18
Strain	I	/	/	1, 2, 3, 4, 5	/	/	2, 4
	II	/	/	2, 4	/	/	2, 4
	III	/	/	/	/	/	/
	IV	/	/	/	/	/	4
The number of measurements		10	0	17	16	0	21

Table 2 Comparison of the identified Young's modulus (GPa) from Set 1

Section	Case 1		Case3	
	Identified	Bias	Identified	Bias
①	34.15	-0.85	34.15	-0.85
②	34.43	-0.57	34.51	-0.49
③	35.75	0.75	35.71	0.71
④	34.74	-0.26	34.75	-0.25
⑤	34.74	-0.26	34.75	-0.25
⑥	35.75	0.75	35.71	0.71
⑦	34.43	-0.58	34.51	-0.49
⑧	34.15	-0.85	34.14	-0.86
Estimated absolute bias (B)	1.01		1.01	
Average absolute bias	0.61		0.58	
Maximum absolute bias	0.85		0.86	

Based on the true parameters, the optimal sensor placements are obtained by using the proposed heuristic. These results are listed in Table 1, where the sensor position is represented by the cross-section number and the position (I, II, III and IV) on that cross-section. It is noticed that if both displacements and strains are considered (Case 3), the optimized sensor placement will have these two kinds of measurements. If only strains are considered, the program fails to find any good sensor placement (L_Ω is always greater than one for these strain measurements). And the total number of measurements in Case 1 is less than that in Case 3.

Then parameter identifications are carried out based on the optimized sensor placements. Although the sensor placement design is carried out alternatively with the parameter identification, the finally converged sensor placements are the same as the initial ones for these cases, even if the initial parameters are far away from the true parameters. This implies parameter identification results are not sensitive to the initial parameters and for these cases, the initial sensor placements are nearly optimal, since the true parameters are used in the design phase.

The identified parameters are compared in Table 2 and Table 3. It is observed that calculated

Table 3 Comparison of the identified Young's modulus (GPa) from Set 2

Section	Case 1		Case3	
	Identified	Bias	Identified	Bias
①	35.20	0.20	35.18	0.18
②	35.06	0.05	35.02	0.02
③	35.20	0.20	35.20	0.20
④	34.99	-0.01	35.01	0.01
⑤	34.98	-0.02	34.98	-0.02
⑥	34.79	-0.21	34.80	-0.20
⑦	35.04	0.04	35.03	0.02
⑧	34.84	-0.16	34.84	-0.16
Estimated absolute bias (B)	0.23		0.23	
Average absolute bias	0.11		0.10	
Maximum absolute bias	0.21		0.20	

maximum absolute biases are always less than and close to the estimated ones. This means Eq. (14) gives a good estimate of the upper bound of identification biases. More over, the maximum relative identification error is only about 2.5%, which implies that identification procedures are stable. Comparing the maximum absolute bias, Case 3 is a little bit worse than Case 1 in Set 1; while Case 3 is a little bit better than Case 1 in Set 2. That is to say, in some cases using the multi-type sensors may improve the identification quality, and in other cases, this may not give any help. Mind that, the proposed heuristic can find only near optimal sensor placements. If this heuristic can be further improved, the results of Case 1 in Set 1 may be automatically found even if using the candidate measurements as those in Case 3. Therefore, it is beneficial to using multi-type sensors in practice.

4.2 The benefit from Monte Carlo simulation

Since true parameters are unknown in practice, Monte Carlo simulation is carried out to find a reasonable super set of measurements in this example. Let the mean value of Young's modulus is 35GPa, and the standard deviation is 3.5GPa, 50 samples are obtained from the simulation, where the candidate measurements are taken from Case 3 of Set 2 generated in previous example. Two OPs are tried to construct the super measurement set: one is 2% that results in the union of the optimal placements over all samples; another is 35% that results in a smaller super set. These two super sets are denoted as Case 4 and Case 5, respectively.

Table 4 compares the obtained sensor placements for these three cases. It observes that the initial measurements of Case 3 are included in the initial set of case 4, but are not included in the initial set of Case 5. Because the true parameters are not used in the Monte Carlo simulation, in Case 4 and Case 5, the initial sets are not the same as the final sets obtained in the parameter identification procedures. It is further noticed that these final sets are not sensitive to the initial parameters used in the parameter identification procedures.

Table 5 compares the identified parameters among these three cases. It is noticed that these three cases give very good identification results, because the maximum absolute biases are very small. This implies good sensor placement can be estimated by using Monte Carlo simulations, even if

Table 4 The comparison of optimal sensor placements

Measurement		Case 3 (Previous example)		Case 4 (OP = 2%)		Case 5 (OP = 35%)	
		Initial set	Final set	Initial set	Final set	Initial set	Final set
Displacement	I	3, 4, 6, 8, 9, 10, 12, 15, 16	3, 4, 6, 8, 9, 10, 12, 15, 16	2, 3, 4, 5, 6, 7, 8, 9, 10, 11, 12, 13, 15, 16, 17, 18	3, 4, 7, 9, 10, 15, 18	3, 4, 8, 9, 10, 12, 13, 15, 16, 18	3, 4, 8, 9, 10, 12, 13, 16
	II	3, 4, 6, 10, 11, 17, 18	3, 4, 6, 10, 11, 17, 18	2, 3, 4, 5, 6, 7, 8, 9, 10, 11, 12, 13, 15, 16, 17, 18	3, 4, 6, 10, 11, 12, 16, 17	2, 3, 4, 6, 9, 10, 12, 13, 16, 17, 18	3, 4, 9, 12, 13, 17, 18
Strain	I	2, 4	2, 4	1, 2, 4	2, 4	2, 4	2, 4
	II	2, 4	2, 4	2, 4	2, 4	2, 4	2, 4
	III	/	/	2	/	/	/
	IV	4	4	2, 4	/	/	/
The number of measurements		21	21	40	19	25	19

Table 5 Comparison of the identified Young's modulus (GPa)

Section	Case 3 (Previous example)		Case 4 (OP = 2%)		Case 5 (OP = 35%)	
	Identified	Bias	Identified	Bias	Identified	Bias
①	35.18	0.18	35.26	0.26	35.08	0.08
②	35.02	0.02	35.07	0.07	34.97	-0.03
③	35.20	0.20	35.28	0.28	35.08	0.08
④	35.01	0.01	34.94	-0.06	35.14	0.14
⑤	34.98	-0.02	35.04	0.03	34.85	-0.15
⑥	34.80	-0.20	34.72	-0.28	34.82	-0.18
⑦	35.03	0.02	35.01	0.01	34.90	-0.10
⑧	34.84	-0.16	34.75	-0.25	34.95	-0.05
Estimated absolute bias	0.23		/		/	
Average absolute bias	0.10		0.16		0.10	
Maximum absolute bias	0.20		0.28		0.18	

true parameters are unknown. Moreover, because the parameter identification and the sensor designing are carried out alternatively, the identified parameters are not sensitive to the initial parameters and the redundancy of sensor placement can be naturally considered.

However, it further observes that the worse result comes from Case 4, although whose initial set covers the initial sets of other two cases; the best result comes from Case 5, although the number of measurements of Case 5 is the smallest among these three cases. These unusual observations indicate that only near optimal solution can be found by the proposed heuristic and further improvement is needed in the future.

5. Conclusions

This paper presents a new heuristic to design the optimal sensor placement. Since the true parameters are unknown in the design phase, Monte Carlo simulation is proposed to obtain a reasonable super measurements set. Based on these candidate measurements, the parameter identification is carried out together with the sensor placement design. Both the sensor placement design and the parameter identification can consider the multi-type sensors.

The validity of the proposed algorithms is illustrated by two bridge examples. It observes that it is beneficial to using multi-type sensors in practice and Monte Carlo simulations can give very good candidate measurements. Because the parameter identification starts from a super measurement set and will be conducted alternatively with sensor design heuristic, the identified parameters are not sensitive to the initial parameters and the redundancy of the sensor placement can be naturally considered.

It is noted that the optimal sensor placement is dependent on loading cases. If there are multipul truck loadings in practice, the proposed algorithms are still valid, provided that a super measurement set should be constructed from the Monte Carlo simulation over all loading cases.

In addition, although the proposed heuristic can give satisfactory results, further improvement on the heuristic of combinatorial optimization still need in the future work.

Acknowledgements

This research is conducted under the contract "Damage detection and sensor placement design for bridge health monitoring systems" from CCCC Highway and Bridge Consultants Co., Ltd. This support is gratefully acknowledged.

References

Sohn, H., Farrar, C.R., Francois, M.H., Devin, D.S., Damiel, W.S. and Brett, R.N. (2003), A review of structural health monitoring literature: 1996-2001. Los Alamos National Laboratory, New Mexico, 2003, Rep. LA-13976-MS.

Yusuke, H., Lie, W.T. and Soumitra, G. (1994), "Inverse analysis of an embankment on soft clay by extended Bayesian method", *Int. J. Numeri. Analy. Methods Geomecha.*, **18**, 709-734.

Zhou, M.S., Li, Y.Q., Xiang, Z.H., Swoboda, G. and Cen, Z.Z. (2007), "A modified extended Bayesian method for damage estimation", *Tsinghua Science and Technology*, **12**, 546-553.

Kammer, D.C. (1991), "Sensor placement for on-orbit modal identification and correlation of large space structures", *J. Guidance, Control Dyn.*, **14**, 251-259.

Heo, G., Wang, M.L. and Satpathi, D. (1997), "Optimal transducer placement for health monitoring of long span bridge", *Soil Dyn. Earthq. Eng.*, **6**, 495-502.

Haftka, R.T. and Scott, E.P., (1998), "Cruz JR. Optimization and experiments: a survey", *Appl. Mech. Reviews*, **51**, 435-448.

Padula, S.L. and Kincaid, R.K. (1999), "Optimization strategies for sensor and actuator placement", Technical report TM-1999-209126, National Aeronautics and Space Administration, Virginia.

Li, G., Qin, Q. and Dong, C. (2000), "Optimal placement of sensors for monitoring systems on suspension bridges using genetic algorithms", *Eng. Mech.*, **17**, 25-34 (in Chinese).

Worden, K. and Burrows, A.P. (2001), "Optimal sensor placement for fault detection", *Eng. Struct.*, **23**, 885-901.

Xiang, Z.H., Swoboda, G. and Cen, Z.Z. (2003), "On the optimal layout of displacement measurements for parameter identification process in geomechanics", *ASCE The Int. J. Geomech.*, **3**, 205-216.
Sanayei, M. and Onipede, O. (1991), "Damage assessment of structures using static test data", *AIAA J.*, **29**, 1174-1179.
Banan, M.R. and Hjelmstad, K.D. (1994), "Parameter estimation of structures from static response I: computational aspects", *J. Struct. Eng.*, **120**, 3243-3258.
Banan, M.R. and Hjelmstad, K.D. (1994), "Parameter estimation of structures from static response II: numerical simulation studies", *J. Struct. Eng.*, **120**, 3259-3283.
Liu, P.L. and Chian, C.C. (1997), "Parameter identification of truss structures using static strains", *J. Struct. Eng.*, **123**, 927-933.
Cui, F., Yuan, W.C. and Shi, J.J. (2000), "Damage detection of structures based on static response", *J. Tongji University*, **28**, 5-8 (in Chinese).
Li, Y.Q., Xiang, Z.H., Zhou, M.S. and Cen, Z.Z., "An integrated parameter identification method combined with sensor placement design", *Communications in Numerical Methods in Engineering* (in press, published online, DOI: 10.1002/cnm.1052).